Search for the reaction $e^+e^- \to \chi_{cJ}\pi^+\pi^-$ and a charmoniumlike structure decaying to $\chi_{cJ}\pi^\pm$ between 4.18 and 4.60 GeV

M. Ablikim,[1] M. N. Achasov,[10,c] P. Adlarson,[64] S. Ahmed,[15] M. Albrecht,[4] A. Amoroso,[63a,63c] Q. An,[60,48] Anita,[21] Y. Bai,[47] O. Bakina,[29] R. Baldini Ferroli,[23a] I. Balossino,[24a] Y. Ban,[38,k] K. Begzsuren,[26] J. V. Bennett,[5] N. Berger,[28] M. Bertani,[23a] D. Bettoni,[24a] F. Bianchi,[63a,63c] J. Biernat,[64] J. Bloms,[57] A. Bortone,[63a,63c] I. Boyko,[29] R. A. Briere,[5] H. Cai,[65] X. Cai,[1,48] A. Calcaterra,[23a] G. F. Cao,[1,52] N. Cao,[1,52] S. A. Cetin,[51b] J. F. Chang,[1,48] W. L. Chang,[1,52] G. Chelkov,[29,b] D. Y. Chen,[6] G. Chen,[1] H. S. Chen,[1,52] M. L. Chen,[1,48] S. J. Chen,[36] X. R. Chen,[25] Y. B. Chen,[1,48] W. S. Cheng,[63c] G. Cibinetto,[24a] F. Cossio,[63c] X. F. Cui,[37] H. L. Dai,[1,48] J. P. Dai,[42,g] X. C. Dai,[1,52] A. Dbeyssi,[15] R. B. de Boer,[4] D. Dedovich,[29] Z. Y. Deng,[1] A. Denig,[28] I. Denysenko,[29] M. Destefanis,[63a,63c] F. De Mori,[63a,63c] Y. Ding,[34] C. Dong,[37] J. Dong,[1,48] L. Y. Dong,[1,52] M. Y. Dong,[1,48,52] S. X. Du,[68] J. Fang,[1,48] S. S. Fang,[1,52] Y. Fang,[1] R. Farinelli,[24a] L. Fava,[63b,63c] F. Feldbauer,[4] G. Felici,[23a] C. Q. Feng,[60,48] M. Fritsch,[4] C. D. Fu,[1] Y. Fu,[1] X. L. Gao,[60,48] Y. Gao,[61] Y. Gao,[38,k] Y. G. Gao,[6] I. Garzia,[24a,24b] E. M. Gersabeck,[55] A. Gilman,[56] K. Goetzen,[11] L. Gong,[37] W. X. Gong,[1,48] W. Gradl,[28] M. Greco,[63a,63c] L. M. Gu,[36] M. H. Gu,[1,48] S. Gu,[2] Y. T. Gu,[13] C. Y. Guan,[1,52] A. Q. Guo,[22] L. B. Guo,[35] R. P. Guo,[40] Y. P. Guo,[28] Y. P. Guo,[9,h] A. Guskov,[29] S. Han,[65] T. T. Han,[41] T. Z. Han,[9,h] X. Q. Hao,[16] F. A. Harris,[53] K. L. He,[1,52] F. H. Heinsius,[4] T. Held,[4] Y. K. Heng,[1,48,52] M. Himmelreich,[11,f] T. Holtmann,[4] Y. R. Hou,[52] Z. L. Hou,[1] H. M. Hu,[1,52] J. F. Hu,[42,g] T. Hu,[1,48,52] Y. Hu,[1] G. S. Huang,[60,48] L. Q. Huang,[61] X. T. Huang,[41] Z. Huang,[38,k] N. Huesken,[57] T. Hussain,[62] W. Ikegami Andersson,[64] W. Imoehl,[22] M. Irshad,[60,48] S. Jaeger,[4] S. Janchiv,[26,j] Q. Ji,[1] Q. P. Ji,[16] X. B. Ji,[1,52] X. L. Ji,[1,48] H. B. Jiang,[41] X. S. Jiang,[1,48,52] X. Y. Jiang,[37] J. B. Jiao,[41] Z. Jiao,[18] S. Jin,[36] Y. Jin,[54] T. Johansson,[64] N. Kalantar-Nayestanaki,[31] X. S. Kang,[34] R. Kappert,[31] M. Kavatsyuk,[31] B. C. Ke,[43,1] I. K. Keshk,[4] A. Khoukaz,[57] P. Kiese,[28] R. Kiuchi,[1] R. Kliemt,[11] L. Koch,[30] O. B. Kolcu,[51b,e] B. Kopf,[4] M. Kuemmel,[4] M. Kuessner,[4] A. Kupsc,[64] M. G. Kurth,[1,52] W. Kühn,[30] J. J. Lane,[55] J. S. Lange,[30] P. Larin,[15] L. Lavezzi,[63c] H. Leithoff,[28] M. Lellmann,[28] T. Lenz,[28] C. Li,[39] C. H. Li,[33] Cheng Li,[60,48] D. M. Li,[68] F. Li,[1,48] G. Li,[1] H. B. Li,[1,52] H. J. Li,[9,h] J. L. Li,[41] J. Q. Li,[4] Ke Li,[1] L. K. Li,[1] Lei Li,[3] P. L. Li,[60,48] P. R. Li,[32] S. Y. Li,[50] W. D. Li,[1,52] W. G. Li,[1] X. H. Li,[60,48] X. L. Li,[41] Z. B. Li,[49] Z. Y. Li,[49] H. Liang,[60,48] H. Liang,[1,52] Y. F. Liang,[45] Y. T. Liang,[25] L. Z. Liao,[1,52] J. Libby,[21] C. X. Lin,[49] B. Liu,[42,g] B. J. Liu,[1] C. X. Liu,[1] D. Liu,[60,48] D. Y. Liu,[42,g] F. H. Liu,[44] Fang Liu,[1] Feng Liu,[6] H. B. Liu,[13] H. M. Liu,[1,52] Huanhuan Liu,[1] Huihui Liu,[17] J. B. Liu,[60,48] J. Y. Liu,[1,52] K. Liu,[1] K. Y. Liu,[34] Ke Liu,[6] L. Liu,[60,48] Q. Liu,[52] S. B. Liu,[60,48] Shuai Liu,[46] T. Liu,[1,52] X. Liu,[32] Y. B. Liu,[37] Z. A. Liu,[1,48,52] Z. Q. Liu,[41] Y. F. Long,[38,k] X. C. Lou,[1,48,52] F. X. Lu,[16] H. J. Lu,[18] J. D. Lu,[1,52] J. G. Lu,[1,48] X. L. Lu,[1] Y. Lu,[1] Y. P. Lu,[1,48] C. L. Luo,[35] M. X. Luo,[67] P. W. Luo,[49] T. Luo,[9,h] X. L. Luo,[1,48] S. Lusso,[63c] X. R. Lyu,[52] F. C. Ma,[34] H. L. Ma,[1] L. L. Ma,[41] M. M. Ma,[1,52] Q. M. Ma,[1] R. Q. Ma,[1,52] R. T. Ma,[52] X. N. Ma,[37] X. X. Ma,[1,52] X. Y. Ma,[1,48] Y. M. Ma,[41] F. E. Maas,[15] M. Maggiora,[63a,63c] S. Maldaner,[28] S. Malde,[58] Q. A. Malik,[62] A. Mangoni,[23b] Y. J. Mao,[38,k] Z. P. Mao,[1] S. Marcello,[63a,63c] Z. X. Meng,[54] J. G. Messchendorp,[31] G. Mezzadri,[24a] T. J. Min,[36] R. E. Mitchell,[22] X. H. Mo,[1,48,52] Y. J. Mo,[6] N. Yu. Muchnoi,[10,c] H. Muramatsu,[56] S. Nakhoul,[11,f] Y. Nefedov,[29] F. Nerling,[11,f] I. B. Nikolaev,[10,c] Z. Ning,[1,48] S. Nisar,[8,i] S. L. Olsen,[52] Q. Ouyang,[1,48,52] S. Pacetti,[23b] X. Pan,[46] Y. Pan,[55] A. Pathak,[1] P. Patteri,[23a] M. Pelizaeus,[4] H. P. Peng,[60,48] K. Peters,[11,f] J. Pettersson,[64] J. L. Ping,[35] R. G. Ping,[1,52] A. Pitka,[4] R. Poling,[56] V. Prasad,[60,48] H. Qi,[60,48] H. R. Qi,[50] M. Qi,[36] T. Y. Qi,[2] S. Qian,[1,48] W.-B. Qian,[52] Z. Qian,[49] C. F. Qiao,[52] L. Q. Qin,[12] X. P. Qin,[13] X. S. Qin,[4] Z. H. Qin,[1,48] J. F. Qiu,[1] S. Q. Qu,[37] K. H. Rashid,[62] K. Ravindran,[21] C. F. Redmer,[28] A. Rivetti,[63c] V. Rodin,[31] M. Rolo,[63c] G. Rong,[1,52] Ch. Rosner,[15] M. Rump,[57] A. Sarantsev,[29,d] Y. Schelhaas,[28] C. Schnier,[4] K. Schoenning,[64] D. C. Shan,[46] W. Shan,[19] X. Y. Shan,[60,48] M. Shao,[60,48] C. P. Shen,[2] P. X. Shen,[37] X. Y. Shen,[1,52] H. C. Shi,[60,48] R. S. Shi,[1,52] X. Shi,[1,48] X. D. Shi,[60,48] J. J. Song,[41] Q. Q. Song,[60,48] W. M. Song,[27] Y. X. Song,[38,k] S. Sosio,[63a,63c] S. Spataro,[63a,63c] F. F. Sui,[41] G. X. Sun,[1] J. F. Sun,[16] L. Sun,[65] S. S. Sun,[1,52] T. Sun,[1,52] W. Y. Sun,[35] Y. J. Sun,[60,48] Y. K. Sun,[60,48] Y. Z. Sun,[1] Z. T. Sun,[1] Y. H. Tan,[65] Y. X. Tan,[60,48] C. J. Tang,[45] G. Y. Tang,[1] J. Tang,[49] V. Thoren,[64] B. Tsednee,[26] I. Uman,[51d] B. Wang,[1] B. L. Wang,[52] C. W. Wang,[36] D. Y. Wang,[38,k] H. P. Wang,[1,52] K. Wang,[1,48] L. L. Wang,[1] M. Wang,[41] M. Z. Wang,[38,k] Meng Wang,[1,52] W. H. Wang,[65] W. P. Wang,[60,48] X. Wang,[38,k] X. F. Wang,[32] X. L. Wang,[9,h] Y. Wang,[49] Y. Wang,[60,48] Y. D. Wang,[15] Y. F. Wang,[1,48,52] Y. Q. Wang,[1] Z. Wang,[1,48] Z. Y. Wang,[1] Ziyi Wang,[52] Zongyuan Wang,[1,52] D. H. Wei,[12] P. Weidenkaff,[28] F. Weidner,[57] S. P. Wen,[1] D. J. White,[55] U. Wiedner,[4] G. Wilkinson,[58] M. Wolke,[64] L. Wollenberg,[4] J. F. Wu,[1,52] L. H. Wu,[1] L. J. Wu,[1,52] X. Wu,[9,h] Z. Wu,[1,48] L. Xia,[60,48] H. Xiao,[9,h] S. Y. Xiao,[1] Y. J. Xiao,[1,52] Z. J. Xiao,[35] X. H. Xie,[38,k] Y. G. Xie,[1,48] Y. H. Xie,[6] T. Y. Xing,[1,52] X. A. Xiong,[1,52] G. F. Xu,[1] J. J. Xu,[36] Q. J. Xu,[14] W. Xu,[1,52] X. P. Xu,[46] L. Yan,[9,h] L. Yan,[63a,63c] W. B. Yan,[60,48] W. C. Yan,[68] Xu Yan,[46] H. J. Yang,[42,g] H. X. Yang,[1] L. Yang,[65] R. X. Yang,[60,48] S. L. Yang,[1,52] Y. H. Yang,[36] Y. X. Yang,[12] Yifan Yang,[1,52] Zhi Yang,[25] M. Ye,[1,48] M. H. Ye,[7] J. H. Yin,[1] Z. Y. You,[49] B. X. Yu,[1,48,52] C. X. Yu,[37] G. Yu,[1,52] J. S. Yu,[20,l] T. Yu,[61] C. Z. Yuan,[1,52] W. Yuan,[63a,63c] X. Q. Yuan,[38,k] Y. Yuan,[1] Z. Y. Yuan,[49] C. X. Yue,[33] A. Yuncu,[51b,a] A. A. Zafar,[62] Y. Zeng,[20,l] B. X. Zhang,[1] Guangyi Zhang,[16] H. H. Zhang,[49] H. Y. Zhang,[1,48] J. L. Zhang,[66] J. Q. Zhang,[4] J. W. Zhang,[1,48,52] J. Y. Zhang,[1] J. Z. Zhang,[1,52] Jianyu Zhang,[1,52] Jiawei Zhang,[1,52] L. Zhang,[1] Lei Zhang,[36] S. Zhang,[49]

S. F. Zhang,[36] T. J. Zhang,[42,g] X. Y. Zhang,[41] Y. Zhang,[58] Y. H. Zhang,[1,48] Y. T. Zhang,[60,48] Yan Zhang,[60,48] Yao Zhang,[1] Yi Zhang,[9,h] Z. H. Zhang,[6] Z. Y. Zhang,[65] G. Zhao,[1] J. Zhao,[33] J. Y. Zhao,[1,52] J. Z. Zhao,[1,48] Lei Zhao,[60,48] Ling Zhao,[1] M. G. Zhao,[37] Q. Zhao,[1] S. J. Zhao,[68] Y. B. Zhao,[1,48] Y. X. Zhao Zhao,[25] Z. G. Zhao,[60,48] A. Zhemchugov,[29,b] B. Zheng,[61] J. P. Zheng,[1,48] Y. Zheng,[38,k] Y. H. Zheng,[52] B. Zhong,[35] C. Zhong,[61] L. P. Zhou,[1,52] Q. Zhou,[1,52] X. Zhou,[65] X. K. Zhou,[52] X. R. Zhou,[60,48] A. N. Zhu,[1,52] J. Zhu,[37] K. Zhu,[1] K. J. Zhu,[1,48,52] S. H. Zhu,[59] W. J. Zhu,[37] X. L. Zhu,[50] Y. C. Zhu,[60,48] Z. A. Zhu,[1,52] B. S. Zou,[1] and J. H. Zou[1]

(BESIII Collaboration)

[1]*Institute of High Energy Physics, Beijing 100049, People's Republic of China*
[2]*Beihang University, Beijing 100191, People's Republic of China*
[3]*Beijing Institute of Petrochemical Technology, Beijing 102617, People's Republic of China*
[4]*Bochum Ruhr-University, D-44780 Bochum, Germany*
[5]*Carnegie Mellon University, Pittsburgh, Pennsylvania 15213, USA*
[6]*Central China Normal University, Wuhan 430079, People's Republic of China*
[7]*China Center of Advanced Science and Technology, Beijing 100190, People's Republic of China*
[8]*COMSATS University Islamabad, Lahore Campus, Defence Road, Off Raiwind Road, 54000 Lahore, Pakistan*
[9]*Fudan University, Shanghai 200443, People's Republic of China*
[10]*G.I. Budker Institute of Nuclear Physics SB RAS (BINP), Novosibirsk 630090, Russia*
[11]*GSI Helmholtzcentre for Heavy Ion Research GmbH, D-64291 Darmstadt, Germany*
[12]*Guangxi Normal University, Guilin 541004, People's Republic of China*
[13]*Guangxi University, Nanning 530004, People's Republic of China*
[14]*Hangzhou Normal University, Hangzhou 310036, People's Republic of China*
[15]*Helmholtz Institute Mainz, Johann-Joachim-Becher-Weg 45, D-55099 Mainz, Germany*
[16]*Henan Normal University, Xinxiang 453007, People's Republic of China*
[17]*Henan University of Science and Technology, Luoyang 471003, People's Republic of China*
[18]*Huangshan College, Huangshan 245000, People's Republic of China*
[19]*Hunan Normal University, Changsha 410081, People's Republic of China*
[20]*Hunan University, Changsha 410082, People's Republic of China*
[21]*Indian Institute of Technology Madras, Chennai 600036, India*
[22]*Indiana University, Bloomington, Indiana 47405, USA*
[23a]*INFN Laboratori Nazionali di Frascati, I-00044, Frascati, Italy*
[23b]*INFN and University of Perugia, I-06100, Perugia, Italy*
[24a]*INFN Sezione di Ferrara, I-44122, Ferrara, Italy*
[24b]*University of Ferrara, I-44122, Ferrara, Italy*
[25]*Institute of Modern Physics, Lanzhou 730000, People's Republic of China*
[26]*Institute of Physics and Technology, Peace Ave. 54B, Ulaanbaatar 13330, Mongolia*
[27]*Jilin University, Changchun 130012, People's Republic of China*
[28]*Johannes Gutenberg University of Mainz, Johann-Joachim-Becher-Weg 45, D-55099 Mainz, Germany*
[29]*Joint Institute for Nuclear Research, 141980 Dubna, Moscow region, Russia*
[30]*Justus-Liebig-Universitaet Giessen, II. Physikalisches Institut, Heinrich-Buff-Ring 16, D-35392 Giessen, Germany*
[31]*KVI-CART, University of Groningen, NL-9747 AA Groningen, The Netherlands*
[32]*Lanzhou University, Lanzhou 730000, People's Republic of China*
[33]*Liaoning Normal University, Dalian 116029, People's Republic of China*
[34]*Liaoning University, Shenyang 110036, People's Republic of China*
[35]*Nanjing Normal University, Nanjing 210023, People's Republic of China*
[36]*Nanjing University, Nanjing 210093, People's Republic of China*
[37]*Nankai University, Tianjin 300071, People's Republic of China*
[38]*Peking University, Beijing 100871, People's Republic of China*
[39]*Qufu Normal University, Qufu 273165, People's Republic of China*
[40]*Shandong Normal University, Jinan 250014, People's Republic of China*
[41]*Shandong University, Jinan 250100, People's Republic of China*
[42]*Shanghai Jiao Tong University, Shanghai 200240, People's Republic of China*
[43]*Shanxi Normal University, Linfen 041004, People's Republic of China*
[44]*Shanxi University, Taiyuan 030006, People's Republic of China*
[45]*Sichuan University, Chengdu 610064, People's Republic of China*
[46]*Soochow University, Suzhou 215006, People's Republic of China*

[47]*Southeast University, Nanjing 211100, People's Republic of China*
[48]*State Key Laboratory of Particle Detection and Electronics, Beijing 100049, Hefei 230026, People's Republic of China*
[49]*Sun Yat-Sen University, Guangzhou 510275, People's Republic of China*
[50]*Tsinghua University, Beijing 100084, People's Republic of China*
[51a]*Ankara University, 06100 Tandogan, Ankara, Turkey*
[51b]*Istanbul Bilgi University, 34060 Eyup, Istanbul, Turkey*
[51c]*Uludag University, 16059 Bursa, Turkey*
[51d]*Near East University, Nicosia, North Cyprus, Mersin 10, Turkey*
[52]*University of Chinese Academy of Sciences, Beijing 100049, People's Republic of China*
[53]*University of Hawaii, Honolulu, Hawaii 96822, USA*
[54]*University of Jinan, Jinan 250022, People's Republic of China*
[55]*University of Manchester, Oxford Road, Manchester, M13 9PL, United Kingdom*
[56]*University of Minnesota, Minneapolis, Minnesota 55455, USA*
[57]*University of Muenster, Wilhelm-Klemm-Str. 9, 48149 Muenster, Germany*
[58]*University of Oxford, Keble Rd, Oxford, United Kingdom OX13RH*
[59]*University of Science and Technology Liaoning, Anshan 114051, People's Republic of China*
[60]*University of Science and Technology of China, Hefei 230026, People's Republic of China*
[61]*University of South China, Hengyang 421001, People's Republic of China*
[62]*University of the Punjab, Lahore-54590, Pakistan*
[63a]*University of Turin, I-10125, Turin, Italy*
[63b]*University of Eastern Piedmont, I-15121, Alessandria, Italy*
[63c]*INFN, I-10125, Turin, Italy*
[64]*Uppsala University, Box 516, SE-75120 Uppsala, Sweden*
[65]*Wuhan University, Wuhan 430072, People's Republic of China*
[66]*Xinyang Normal University, Xinyang 464000, People's Republic of China*
[67]*Zhejiang University, Hangzhou 310027, People's Republic of China*
[68]*Zhengzhou University, Zhengzhou 450001, People's Republic of China*

(Received 7 December 2020; accepted 18 February 2021; published 22 March 2021)

We search for the process $e^+e^- \to \chi_{cJ}\pi^+\pi^-$ ($J = 0, 1, 2$) and for a charged charmoniumlike state in the $\chi_{cJ}\pi^\pm$ subsystem. The search uses datasets collected with the BESIII detector at the BEPCII storage ring at center-of-mass energies between 4.18 GeV and 4.60 GeV. No significant $\chi_{cJ}\pi^+\pi^-$ signals are observed at any center-of-mass energy, and thus upper limits are provided which also serve as limits for a possible charmoniumlike structure in the invariant $\chi_{cJ}\pi^\pm$ mass.

DOI: 10.1103/PhysRevD.103.052010

[a]Also at Bogazici University, 34342 Istanbul, Turkey.
[b]Also at the Moscow Institute of Physics and Technology, Moscow 141700, Russia.
[c]Also at the Novosibirsk State University, Novosibirsk, 630090, Russia.
[d]Also at the NRC "Kurchatov Institute", PNPI, 188300, Gatchina, Russia.
[e]Also at Istanbul Arel University, 34295 Istanbul, Turkey.
[f]Also at Goethe University Frankfurt, 60323 Frankfurt am Main, Germany.
[g]Also at Key Laboratory for Particle Physics, Astrophysics and Cosmology, Ministry of Education; Shanghai Key Laboratory for Particle Physics and Cosmology; Institute of Nuclear and Particle Physics, Shanghai 200240, People's Republic of China.
[h]Also at Key Laboratory of Nuclear Physics and Ion-beam Application (MOE) and Institute of Modern Physics, Fudan University, Shanghai 200443, People's Republic of China.
[i]Also at Harvard University, Department of Physics, Cambridge, Massachusetts 02138, USA.
[j]Currently at: Institute of Physics and Technology, Peace Ave.54B, Ulaanbaatar 13330, Mongolia.
[k]Also at State Key Laboratory of Nuclear Physics and Technology, Peking University, Beijing 100871, People's Republic of China.
[l]School of Physics and Electronics, Hunan University, Changsha 410082, China.

I. INTRODUCTION

In the past decade, the discovery of new and exotic resonances has opened up exciting possibilities for further study of quantum chromodynamics in the charmonium and bottomonium energy regions [1–3]. One important resonance is the $Y(4260)$, which was observed by the *BABAR* collaboration in the initial state radiation (ISR) process $e^+e^- \to \gamma_{\rm ISR} J/\psi\pi^+\pi^-$ [4,5] and was confirmed by several other collaborations, such as CLEO [6], Belle [7,8] and BESIII [9]. Despite lying above several open-charm thresholds (starting at 3.73 GeV/c^2), the $Y(4260)$ state, with quantum number $J^{PC} = 1^{--}$, unconventionally couples much more strongly to the final state $J/\psi\pi^+\pi^-$ [10] rather than to open-charm final states. This unexpected behavior has stimulated much interest in the hadron-spectroscopy community.

In 2008, the Belle collaboration, studying the decay $\bar{B}^0 \to K^-\pi^+\chi_{c1}$, observed two charged charmoniumlike structures in the $\chi_{c1}\pi^\pm$ subsystem with a statistical significance of 5σ. These structures were denoted as the $Z_c(4050)^\pm$ and the $Z_c(4250)^\pm$, with masses of $4051 \pm 14^{+20}_{-41}$ MeV/c^2 and $4248^{+44+180}_{-29-35}$ MeV/c^2, respectively, and corresponding widths of 82^{+21+47}_{-17-22} and $177^{+54+316}_{-39-61}$ MeV [11]. This observation was not confirmed by *BABAR*, who set 90% confidence level on the presence of these intermediate states [12]. The first charged charmonium-structure to be found was the $Z(4430)^\pm$ decaying to $\psi(2S)\pi^\pm$, observed by Belle [13], whose resonance nature was established by the LHCb collaboration [14]. The presence of an electric charge indicates a possible internal structure of at least four quarks.

In order to gain additional insight into these states, we perform a search for the $Z_c(4050)^\pm$ in e^+e^- production using data collected by the BESIII experiment at center-of-mass energies between 4.18 GeV/c^2 and 4.60 GeV/c^2. The observation of other charged charmoniumlike states, such as the $Z_c(3900)^\pm$ in $J/\psi\pi^+\pi^-$ [9] and $Z_c(4020)^\pm$ in $h_c\pi^+\pi^-$ [15] in some of these data samples, make the BESIII experiment an ideal environment for the search for exotic particles. In this paper the reaction channels $e^+e^- \to \chi_{cJ}\pi^+\pi^-$ ($J = 0, 1, 2$) are investigated, in which the $Z_c(4050)^\pm$ resonance is expected to appear as a structure in the $\chi_{cJ}\pi^\pm$ invariant-mass spectrum. Due to phase-space restrictions, the production of the second state $Z_c(4250)^\pm$ is only possible at higher energies.

II. EXPERIMENTAL DATA AND MONTE CARLO SAMPLES

The BESIII detector is a magnetic spectrometer [16] located at the Beijing Electron Positron Collider (BEPCII) [17]. The cylindrical core of the BESIII detector consists of a helium-based multilayer drift chamber (MDC), a plastic scintillator time-of-flight system (TOF), and a CsI(Tl) electromagnetic calorimeter (EMC), which are all enclosed in a superconducting solenoidal magnet providing a 1.0 T magnetic field. The solenoid is supported by an octagonal flux-return yoke with resistive plate chamber muon-identifier modules interleaved with steel. The acceptance for charged particles and photons is 93% over the 4π solid angle. The charged-particle momentum resolution at 1 GeV/c is 0.5%, and the dE/dx resolution is 6% for electrons from Bhabha scattering. The EMC measures photon energies with a resolution of 2.5% (5%) at 1 GeV in the barrel (endcap) region. The time resolution of the TOF barrel part is 68 ps. The time resolution of the end-cap TOF system was upgraded in 2015 with multigap resistive plate chamber technology, providing a time resolution of 60 ps. For data taken before 2015 the time resolution was 110 ps [18,19].

For the determination of reconstruction efficiencies and the estimation of background contributions, several Monte Carlo (MC) simulated data samples were produced with a GEANT4-based [20] MC software package. This includes the geometric description of the BESIII detector and the detector response. The signal channels $e^+e^- \to \chi_{cJ}\pi^+\pi^-$, with $\chi_{cJ} \to \gamma J/\psi$ ($J = 0, 1, 2$) and $J/\psi \to \ell^+\ell^-$, are generated via the KKMC generator [21] for the initial resonance and the event generator EvtGen [22] for subsequent decays, using the phase-space distribution (PHSP). The PHSP model is also assumed for the decay $\chi_{cJ} \to \gamma J/\psi$, and the VLL (vector to lepton lepton) model is used for the $J/\psi \to \ell^+\ell^-$ ($\ell = e,\ \mu$) decay. The generation of final state radiation is handled by the PHOTOS package [23]. The simulation includes the beam-energy spread and initial state radiation (ISR) in the e^+e^- annihilations modeled with the generator KKMC [21]. The inclusive MC samples consist of the production of open-charm processes, the ISR production of vector charmonium (like) states, and the continuum processes incorporated in KKMC [21]. Known decay modes are modeled with EvtGen using branching fractions taken from the Particle Data Group [24], and the remaining unknown decays from the charmonium states with LUNDCHARM [25,26]. The size of these inclusive MC samples is scaled to five times of the integrated luminosity of their respective measured data point, with the exception at 4.18 GeV which has forty times the integrated luminosity.

The datasets studied in the analysis are shown in Table I. Most of the samples correspond to an integrated luminosity $\mathcal{L}$ of around 500 pb^{-1}. The samples taken at the center-of-mass energies of 4.18 GeV, 4.23 GeV, 4.26 GeV and 4.42 GeV are considerably larger.

Studies on MC simulated samples are performed in order to optimize the event selection criteria. For all generated MC simulated signal samples of $e^+e^- \to \chi_{cJ}\pi^+\pi^-$, initial state radiation has been deactivated, except for those samples required for the dedicated investigation of the influence of ISR on the final result. Furthermore, several inclusive MC

TABLE I. Data samples used in this analysis with the corresponding integrated luminosity $\mathcal{L}$ [27].

$\sqrt{s}$ (MeV)	$\mathcal{L}$ (pb^{-1})
4178.00	3194.0
4189.27	526.7
4199.60	526.0
4209.72	517.1
4218.81	514.6
4226.26	1056.4
4235.83	530.3
4243.89	538.1
4257.97	828.4
4266.93	531.1
4277.79	175.7
4358.26	543.9
4415.58	1044.0
4527.14	112.1
4599.53	586.9

samples have been analyzed to identify dominant background contributions. The dominant contributions found in the inclusive MC samples have been exclusively simulated. All generated exclusive MC samples contain 500 000 events.

III. EVENT SELECTION

Several selection criteria are applied in order to perform the particle identification (PID) and the event selection.

Photon candidates are constructed from clusters of energy deposits of at least 25 MeV of energy in the barrel part of the EMC (polar angle region of $|\cos\theta| < 0.80$ with respect to the beam axis) and 50 MeV in the endcap region ($0.86 < |\cos\theta| < 0.92$). The corresponding EMC time is required to be within a window of 700 ns relative to the event start time, and the candidates are requested to be at least 20° away from the nearest charged track to reject EMC hits caused by split-offs of clusters of charged particles.

Charged-track candidates must pass the interaction point within a cylindrical volume, with a radius of 1 cm and length of 10 cm, around the interaction point. Furthermore, due to the limitation of the MDC acceptance, the region close to the beams is excluded by requiring $|\cos\theta_{\text{Track}}| < 0.93$. To distinguish pion candidates from the leptons coming from the J/ψ, a combination of the track momenta measured with the MDC (P_{MDC}) and the energy deposited in the EMC (E_{EMC}) is used. Pion candidates are tracks with a momentum smaller than 1.0 GeV/c and lepton candidates are tracks with a momentum greater than 1.0 GeV/c. Furthermore, to separate the electrons from muons, tracks with a ratio of $E_{\text{EMC}}/P_{\text{MDC}} < 0.3c$ are considered to be muon candidates and tracks with $E_{\text{EMC}}/P_{\text{MDC}} > 0.7c$ are considered as electron candidates.

In order to select $e^+e^- \to \chi_{cJ}\pi^+\pi^-$ events, four track candidates with a net charge of zero, including two lepton candidates, and at least one photon candidate are required. A vertex fit of the tracks to a common vertex is applied. Then, a kinematic fit with constraints on the initial-four-momentum (4C) and the mass of the J/ψ meson (5C-fit) to $m_{J/\psi,\text{PDG}}$ [24] is performed. Candidates that satisfy $\chi^2_{\text{5C}} < 50$ are retained for further analysis. If multiple candidates are found in an event, the one with the lowest χ^2_{5C} value is selected. However, only one candidate is seen after the event selection in signal MC data and predominantly one in data.

IV. BACKGROUND STUDIES

The following processes have been identified as the principal sources of background events through the study of the inclusive Monte Carlo samples:

$e^+e^- \to e^+e^-\gamma_{\text{ISR}}, \gamma_{\text{ISR}} \to e^+e^-$;
$e^+e^- \to \eta J/\psi, \eta \to \gamma\pi^+\pi^-$;
$e^+e^- \to \eta' J/\psi, \eta' \to \gamma\rho^0, \rho^0 \to \pi^+\pi^-$;
$e^+e^- \to \omega\chi_{cJ}, \omega \to \pi^+\pi^-, \chi_{cJ} \to \gamma J/\psi$ $(J = 0, 1, 2)$;
$e^+e^- \to \gamma_{\text{ISR}}\psi(2S), \psi(2S) \to \pi^+\pi^- J/\psi$; and
$e^+e^- \to Y(4260) \to \gamma X(3872), X(3872) \to J/\psi\pi^+\pi^-$.

In all these reactions the J/ψ decays into a lepton pair ($e^+e^-/\mu^+\mu^-$). Apart from the first process, these contributions have the same final state as the signal reaction channel and are thus not distinguishable by the applied kinematic fit. Additional selection criteria based on other kinematic variables are required to suppress these background channels. Background from Bhabha scattering with associated ISR/FSR photons that convert into an electron-positron pair misidentified as a pion pair is suppressed by the requirement that the pion opening angle in the laboratory system, $\alpha^{\pi^+}_{\pi^-}$, satisfies $\cos(\alpha^{\pi^+}_{\pi^-}) < 0.98$. This criterion results in a signal loss below 1% for all studied energy points. The background contributions from $\eta J/\psi$ and $\eta' J/\psi$ are rejected by requiring $m_{\text{rec}} \geq 0.57$ GeV/c^2 and rejecting candidates with $0.95 \leq m_{\text{rec}} \leq 0.97$ GeV/c^2, where m_{rec} is the J/ψ recoil mass. Contamination from $\omega\chi_{cJ}$ events are suppressed by rejecting candidates where the χ_{cJ} recoil mass lies between 0.74 and 0.82 GeV/c^2.

The main ISR background contribution originates from the process $e^+e^- \to \gamma_{\text{ISR}}\psi(2S)$. This reaction is dangerous because the ISR photon has a wide range of possible energies, depending on the center of mass energy. The final source of contamination that is considered is illustrated in Fig. 1, where events that are most likely coming from $\gamma X(3872)$ are confused with $\pi^+\pi^-\chi_{c0}$ signal candidates. Apparent $Y(4260) \to \gamma X(3872)$ events at the center-of-mass energy of 4.18 GeV coincidentally have a photon energy similar to the one coming from a radiative decay of $\chi_{c0} \to \gamma J/\psi$.

Exclusive Monte Carlo datasets containing 500 000 events each are simulated and analyzed for each background process and center-of-mass energy. For $e^+e^- \to \gamma_{\text{ISR}}\psi(2S)$, samples are simulated for each studied center-of-mass

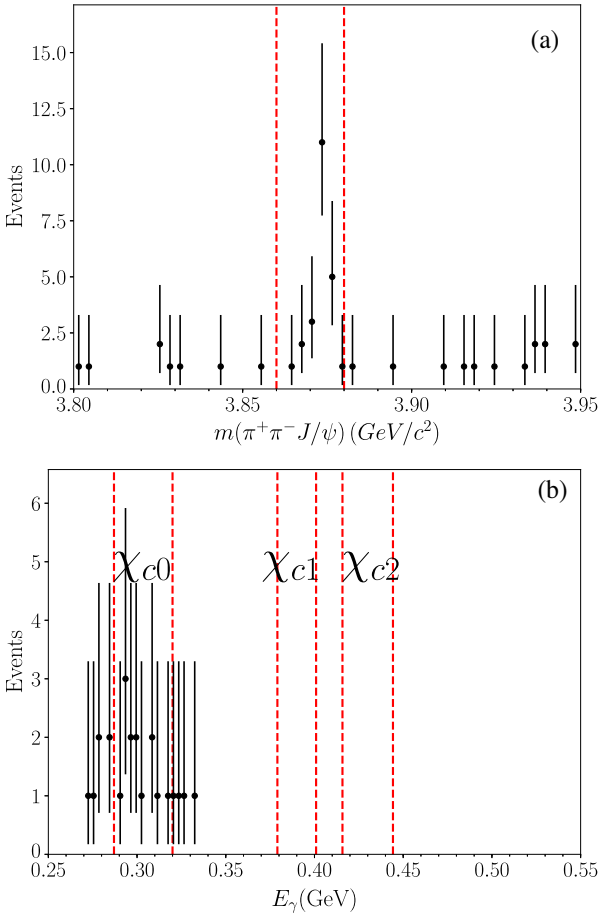

FIG. 1. Contamination from $e^+e^- \to Y(4260) \to \gamma X(3872)$, $X(3872) \to \pi^+\pi^- J/\psi$ events at 4.18 GeV. Plot (a) shows the $X(3872)$ signal, with a selection window indicated by red dashed lines to isolate the events in plot (b), which shows the photon energy. Here, the red dashed lines indicate the χ_{cJ} selection windows.

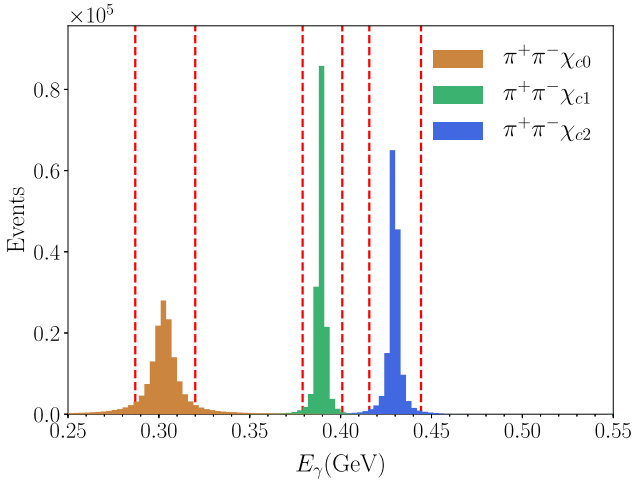

FIG. 2. Reconstructed photon energy E_γ of the χ_{cJ} candidates measured in the rest frame of the $\pi^+\pi^-$ recoil system from generated $\chi_{cJ}\pi^+\pi^-$ Monte Carlo datasets. The red dashed lines indicate the selection windows. The histograms are normalized to the same integral.

energy using KKMC to evaluate the cross section. Events coming from $e^+e^- \to \gamma_{\rm ISR}\psi(2S)/\gamma X(3872)$ with $\psi(2S)/X(3872) \to \pi^+\pi^- J/\psi$ decays are suppressed by rejecting the region $m_{\pi^+\pi^- J/\psi} \le 3.71$ GeV/c^2 and 3.86 GeV/$c^2 \le m_{\pi^+\pi^- J/\psi} \le 3.88$ GeV/c^2, respectively. Due to the restrictions on the phase space, $\omega\chi_{c1}$ and $\omega\chi_{c2}$ contribute only for center-of-mass energies above 4.3 GeV and $\omega\chi_{c0}$ only above 4.2 GeV, respectively.

The reconstruction efficiency is evaluated with simulated MC data of the signal channel. The reconstruction efficiency ranges from 16% to 28% after the application of all selection criteria, depending on the center-of-mass energy (see Tables III–V).

V. CROSS SECTION DETERMINATION

The signal yield is directly determined by counting the events surviving the selection criteria. Since the radiative process $\chi_{cJ} \to \gamma J/\psi$ is a two-body decay, the photon energy of each decay mode serves as a distinctive signature for the separation of the three χ_{cJ} channels. Figure 2 shows the photon energy after boosting it into the $\pi^+\pi^-$ recoil system. This method allows for a clear separation of the three χ_{cJ} channels by setting the (boosted) photon energy windows and leads to the results shown in Tables III to V. There, the first uncertainties are statistical and the second systematic, arising from the sources discussed in Sec. VI. The expected background events for each center-of-mass energy are estimated by adding up each background contribution:

$$N_{\rm bkg} \equiv \mathcal{L}\sum_i \sigma_i \mathcal{B}_i \epsilon_i, \tag{1}$$

where $\mathcal{L}$ is the integrated luminosity at a given center-of-mass energy, σ_i is the cross section for each background contribution, $\mathcal{B}_i$ the corresponding branching ratio and ϵ_i the efficiency from the exclusive background MC data samples after all selection criteria. The values of σ_i are taken from previous BESIII measurements [28–32]. In the cases where no cross section has yet been measured the upper limits are used to provide an estimate. Finally, $\mathcal{B}_i$ is taken from the Particle Data Group (PDG) [24].

The observed cross section $\sigma_{\rm obs}$ is calculated via

$$\sigma_{\rm obs} \equiv \frac{N_{\rm obs} - N_{\rm bkg}}{\mathcal{L}\epsilon\mathcal{B}(\chi_{cJ} \to \gamma J/\psi)\mathcal{B}(J/\psi \to \ell^+\ell^-)}, \tag{2}$$

with the selection efficiency ϵ and $\mathcal{B}(\chi_{cJ} \to \gamma J/\psi)$ being the corresponding branching fraction for the selected χ_{cJ} decay channel and $\mathcal{B}(J/\psi \to \ell^+\ell^-)$ the sum of the two branching fractions $\mathcal{B}(J/\psi \to e^+e^-)$ and $\mathcal{B}(J/\psi \to \mu^+\mu^-)$.

The determination of the upper limits is discussed in further detail in Sec. VIII.

VI. SYSTEMATIC-UNCERTAINTY ESTIMATION

Systematic uncertainties are assigned, where appropriate, for each step and input in the analysis. The uncertainty on the measurement of the integrated luminosity is 1% [27]. The uncertainty on the reconstruction efficiency due to the finite size of the MC simulation sample is 0.3–0.4%. The difference between data and MC simulation of the track and photon reconstruction efficiencies and also the correlation between the tracks are taken into account by assigning a 1% uncertainty per track [33] and per photon [34], resulting in an overall uncertainty of 4.1%. The uncertainty associated with final state radiation is stated to be roughly 0.1% [35] and considered to be negligible.

The uncertainty associated with the selection criteria is assigned to be the largest shift in efficiency observed when the applied criteria are moved by 10% in both directions. For the selection on the χ^2_{5C} of the kinematic fit, this results in an uncertainty of around 1.4%, depending on the center-of-mass energy and applied χ_{cJ} selection. For the η veto the range is much larger and varies between 0.2% and 4.5%.

Similarly, uncertainties associated with other selection criteria also depend on the collision energy. For the background vetoes, the windows are increased and decreased by 10% and again the largest difference, which varies in the range of a few percent, is assigned. In the case of the χ_{c2} selection, the $\psi(2S)$ veto contributes larger systematic uncertainties at lower center-of-mass energies, where the invariant $\pi^+\pi^- J/\psi$ mass of the expected signal lies, coincidentally, in the vicinity of the $\psi(2S)$ mass. The systematic uncertainty is largest for the χ_{c0} selection, on account of the larger natural width of this state.

Table II summarizes the individual systematic uncertainties. Contributions arising from the variation of a certain input from the nominal value are considered to be negligible if the observed change in result is found to be less than the uncorrelated systematic uncertainty. The total systematic uncertainty is calculated as the sum in quadrature of each component, assuming negligible correlations, and results in values between 4.7% to 11.0%. When calculating upper limits, a Gaussian-shaped uncertainty is added to the efficiency with a width equal to the total systematic uncertainty.

VII. ISR CORRECTION

An ISR correction factor is applied to the measured cross section, as listed in Tables III to V. The number of observed events can be written as

$$N = \mathcal{L} \int \sigma(x)\epsilon(x)W(x)dx \qquad (3)$$

TABLE II. Systematic uncertainties separated for the different reaction channels $e^+e^- \to \chi_{cJ}\pi^+\pi^-$. Contributions vary depending on the center-of-mass energy.

Source	$\sigma_{\mathrm{sys}},\chi_{c0}(\%)$	$\sigma_{\mathrm{sys}},\chi_{c1}(\%)$	$\sigma_{\mathrm{sys}},\chi_{c2}(\%)$
Luminosity	1.0	1.0	1.0
Rec. eff.	0.3–0.4	0.3–0.4	0.3–0.4
Track/photon	4.1	4.1	4.1
χ^2-veto	1.3–1.9	1.3–1.7	1.3–1.8
η-veto	0.6–3.7	0.4–2.7	0.2–4.5
$\pi^+\pi^-$-angle	0.4–0.5	0.4–0.5	0.3–0.5
$\psi(2S)$-veto	0.0	0.0–2.4	0.0–9.5
η'-veto	0.2–1.1	0.2–1.2	0.3–1.3
ω-veto	0.3–1.9	0.0–1.8	0.0–1.8
X(3872)-veto	0.0–4.1	0.0–2.8	0.0–2.4
χ_{cJ}-selection	4.7–5.2	0.0–0.0	0.0–0.1
Total	6.9–8.7	4.7–5.9	4.7–11.0

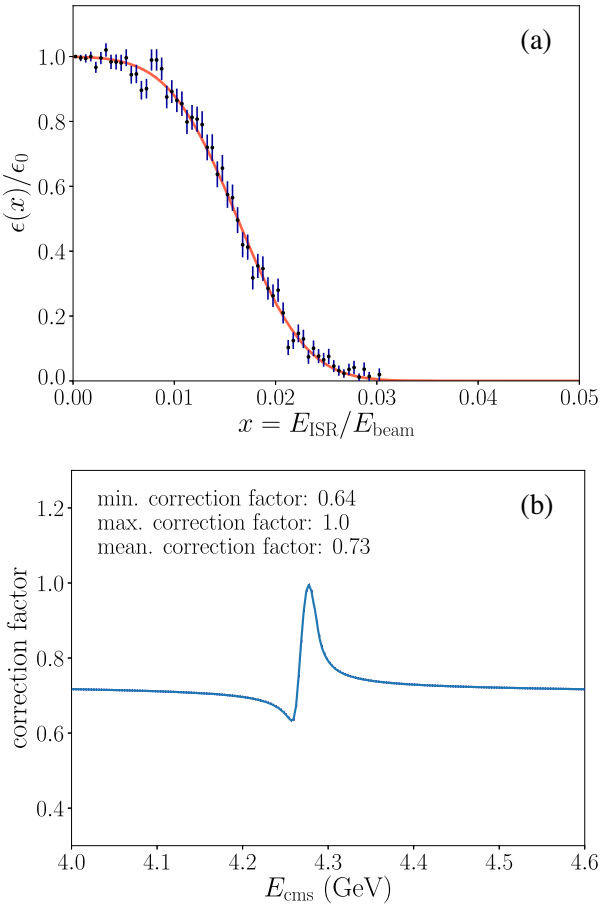

FIG. 3. ISR correction for the reaction channel $e^+e^- \to \pi^+\pi^-\chi_{c1}$ at $E_{\mathrm{cms}} = 4.6$ GeV. (*a*) shows the normalized reconstruction efficiency versus the normalized energy of the ISR photon $E_{\mathrm{ISR}}/E_{\mathrm{beam}}$, where the red curve represents a fit by the error function; (*b*) shows the dependence of the ISR correction factor on E_{cms}, assuming a single narrow resonance with mass of 4.26 GeV/c^2 and width of 10 MeV.

where $x \equiv E_{\rm ISR}/E_{\rm beam}$ and $W(x)$ is the radiator function [36,37]. After factoring out the Born cross section σ_0 and the efficiency ϵ_0 at $x = 0$ this expression becomes

$$N = \mathcal{L}\sigma_0\epsilon_0 \int \frac{\sigma(x)}{\sigma_0}\frac{\epsilon(x)}{\epsilon_0} W(x)dx. \quad (4)$$

The ISR correction factor is defined as

$$\kappa \equiv \int \frac{\sigma(x)}{\sigma_0}\frac{\epsilon(x)}{\epsilon_0} W(x)dx \quad (5)$$

so that

$$N = \mathcal{L}\sigma_0\epsilon_0\kappa. \quad (6)$$

The efficiency ratio $\epsilon(x)/\epsilon_0$ is determined from a sample of MC simulated signal events, which are generated including ISR. Figure 3 *a* shows the efficiency ratio as a function of x for the χ_{c1} signal MC sample at 4.6 GeV. The superimposed fit is an error function, which is found to describe all χ_{cJ} modes and collision energies.

The correction factor κ is strongly correlated to the energy dependence of the signal cross section, which is currently unknown. To obtain conservative upper limits on the signal we estimate the lowest possible κ value. We assume a narrow resonance of width 10 MeV and mass 4.26 GeV/c^2, which results in the κ energy dependence shown in Fig. 3 *b*. Changing the position of the resonance results in a corresponding shift of the κ energy dependence, while the shape is nearly unchanged. The minimal value of the correction factor, $\kappa = 0.64$, is conservatively used to set the upper limits of the cross section at all collision energies.

VIII. UPPER-LIMIT DETERMINATION

The upper limits on the branching ratios are calculated following a frequentist procedure [38,39], using the definition

$$\sigma_{\rm UL} \equiv \frac{N_{\rm UL}}{\mathcal{L}(1+\delta)\frac{1}{|1-\Pi(s)|^2}\epsilon\mathcal{B}}. \quad (7)$$

Here $N_{\rm UL}$ is the upper limit on the signal yield, $\mathcal{L}$ is the integrated luminosity, $(1+\delta) \equiv \kappa$ is the ISR correction factor (see section VII), $\frac{1}{|1-\Pi(s)|^2}$ is the vacuum polarization correction factor (with values in the range 1.05–1.06 from Ref. [40]), ϵ the efficiency from corresponding signal Monte Carlo after selection criteria, and $\mathcal{B}$ is the combined branching ratio of $\mathcal{B}(\chi_{cJ} \to \gamma J/\psi)$ and $\mathcal{B}(J/\psi \to \ell^+\ell^-)$. The systematic uncertainties are taken into account by assuming a Gaussian-shaped uncertainty on the efficiency with a width equal to the total systematic uncertainty.

TABLE III. Measured cross sections and associated information for $e^+e^- \to \chi_{c0}\pi^+\pi^-$ at different center-of mass-energies $E_{\rm cms}$. Shown are the integrated luminosity $\mathcal{L}$, the selection efficiency ϵ, the number of observed events $N_{\rm obs}$, the number of expected background events $N_{\rm bkg}$, the observed cross sections $\sigma_{\rm obs}$ with statistical and systematic uncertainties, the statistical significance and the respective upper limits at 90% confidence level.

$E_{\rm cms}$ (GeV)	$\mathcal{L}$ (pb^{-1})	ϵ(%)	$N_{\rm obs}$	$N_{\rm bkg}$	$\sigma_{\rm obs}$ (pb)	significance (σ)	$\sigma_{\rm UL}$ (pb)
4.178	3194.0	16.21	3	0.0	$3.47^{+3.59}_{-2.26} \pm 0.30$	1.15	11.8
4.189	526.7	16.43	1	0.0	$6.92^{+16.10}_{-6.23} \pm 0.60$	0	37.7
4.200	526.0	16.31	0	0.0	$0^{+8.01}_{-0} \pm 0$	0	20.6
4.210	517.1	16.38	1	0.0	$7.07^{+16.40}_{-6.37} \pm 0.58$	0	38.4
4.219	514.6	16.72	0	0.0	$0^{+7.99}_{-0} \pm 0$	0	20.5
4.226	1056.0	17.01	3	0.0	$9.99^{+10.40}_{-6.50} \pm 0.80$	1.15	34.0
4.236	530.3	18.14	0	0.0	$0^{+7.14}_{-0} \pm 0$	0	18.4
4.244	538.1	19.02	3	0.0	$17.60^{+18.20}_{-11.40} \pm 1.32$	1.15	59.6
4.258	828.4	19.70	2	0.0	$7.34^{+10.00}_{-5.41} \pm 0.55$	0.67	29.1
4.267	531.1	21.10	2	0.0	$10.70^{+14.60}_{-7.88} \pm 0.77$	0.67	42.4
4.278	175.7	21.29	0	0.0	$0^{+18.40}_{-0} \pm 0$	0	47.3
4.358	543.9	21.58	1	0.0	$5.10^{+11.90}_{-4.60} \pm 0.36$	0	27.8
4.416	1044.0	21.86	0	0.0	$0^{+3.01}_{-0} \pm 0$	0	7.8
4.527	112.1	23.85	0	0.0	$0^{+25.70}_{-0} \pm 0$	0	66.1
4.600	586.9	23.92	2	0.0	$8.50^{+11.70}_{-6.29} \pm 0.61$	0.67	33.8

TABLE IV. Measured cross sections and associated information for $e^+e^- \to \chi_{c1}\pi^+\pi^-$. See Table III for more information.

$E_{\rm cms}$ (GeV)	$\mathcal{L}$ (pb^{-1})	$\epsilon(\%)$	$N_{\rm obs}$	$N_{\rm bkg}$	$\sigma_{\rm obs}$ (pb)	significance (σ)	$\sigma_{\rm UL}$ (pb)
4.178	3194.0	26.36	2	0.0	$0.06^{+0.08}_{-0.04} \pm 0$	0.67	0.23
4.189	526.7	27.16	0	0.0	$0^{+0.20}_{-0} \pm 0$	0	0.50
4.200	526.0	27.28	0	0.0	$0^{+0.20}_{-0} \pm 0$	0	0.50
4.210	517.1	27.24	1	0.12	$0.17^{+0.40}_{-0.14} \pm 0$	0	0.94
4.219	514.6	27.24	0	0.0	$0^{+0.2}_{-0} \pm 0$	0	0.51
4.226	1056.4	26.03	4	0.0	$0.36^{+0.28}_{-0.17} \pm 0.02$	1.53	1.09
4.236	530.3	24.71	2	0.0	$0.37^{+0.49}_{-0.24} \pm 0.02$	0.67	1.47
4.244	538.1	23.36	2	0.0	$0.39^{+0.51}_{-0.25} \pm 0.02$	0.67	1.53
4.258	828.4	21.56	2	0.0	$0.27^{+0.36}_{-0.18} \pm 0.02$	0.67	1.08
4.267	531.1	22.32	0	0.0	$0^{+0.24}_{-0} \pm 0$	0	0.61
4.278	175.7	22.19	0	0.0	$0^{+0.72}_{-0} \pm 0$	0	1.85
4.358	543.9	23.48	1	0.0	$0.19^{+0.44}_{-0.16} \pm 0$	0	1.04
4.416	1044.0	25.19	0	0.0	$0^{+0.11}_{-0} \pm 0$	0	0.28
4.527	112.1	27.61	0	0.0	$0^{+0.91}_{-0} \pm 0$	0	2.33
4.600	586.9	27.72	2	0.0	$0.3^{+0.40}_{-0.19} \pm 0.02$	0.67	1.18

The measured cross sections and the corresponding upper limits at the 90% confidence level are summarized in Tables III–V and in Fig. 4. The quoted statistical significance is based on the binomial assumption $Z_{\rm Bi}$, taken from Cousins *et al.* [38] and does not include any systematic uncertainties. With the exception of the channel $e^+e^- \to \pi^+\pi^-\chi_{c1}$, the measured cross sections show no significant variation with center-of-mass energy. It should be noted that the upper limits for $e^+e^- \to \pi^+\pi^-\chi_{c0}$ are less restrictive than those for the other two modes on account of the small branching ratio of $\chi_{c0} \to \gamma J/\psi$. Since no convincing $\chi_{cJ}\pi^+\pi^-$ signal is seen, the quoted upper limits can also be considered as upper limits on the reaction proceeding through a hypothetical $Z_c(4050)^{\pm}$ particle.

TABLE V. Measured cross sections and associated information for $e^+e^- \to \chi_{c2}\pi^+\pi^-$. See Table III for more information.

$E_{\rm cms}$ (GeV)	$\mathcal{L}$ (pb^{-1})	$\epsilon(\%)$	$N_{\rm obs}$	$N_{\rm bkg}$	$\sigma_{\rm obs}$ (pb)	significance (σ)	$\sigma_{\rm UL}$ (pb)
4.178	3194.0	16.90	4	2.02	$0.16^{+0.26}_{-0.16} \pm 0.02$	0.40	0.82
4.189	526.7	19.26	1	0.0	$0.44^{+1.00}_{-0.36} \pm 0.04$	0	2.38
4.200	526.0	21.51	0	0.0	$0^{+0.45}_{-0} \pm 0$	0	1.15
4.210	517.1	23.59	0	0.0	$0^{+0.42}_{-0} \pm 0$	0	1.07
4.219	514.6	25.21	1	0.0	$0.34^{+0.78}_{-0.28} \pm 0.02$	0	1.84
4.226	1056.0	25.61	3	0.0	$0.49^{+0.48}_{-0.27} \pm 0.03$	1.15	1.65
4.236	530.3	27.29	0	0.0	$0^{+0.35}_{-0} \pm 0$	0	0.90
4.244	538.1	27.90	1	0.0	$0.29^{+0.68}_{-0.24} \pm 0.01$	0	1.59
4.258	828.4	26.59	1	0.0	$0.2^{+0.46}_{-0.17} \pm 0.01$	0	1.09
4.267	531.1	27.00	0	0.0	$0^{+0.35}_{-0} \pm 0$	0	0.91
4.278	175.7	25.19	1	0.0	$1.0^{+2.29}_{-0.83} \pm 0.05$	0	5.4
4.358	543.9	21.54	0	0.0	$0^{+0.43}_{-0} \pm 0$	0	1.12
4.416	1044.0	23.91	2	0.0	$0.35^{+0.47}_{-0.23} \pm 0.02$	0.67	1.4
4.527	112.1	27.23	0	0.0	$0^{+1.66}_{-0} \pm 0$	0	4.26
4.600	586.9	27.27	0	0.0	$0^{+0.32}_{-0} \pm 0$	0	0.81

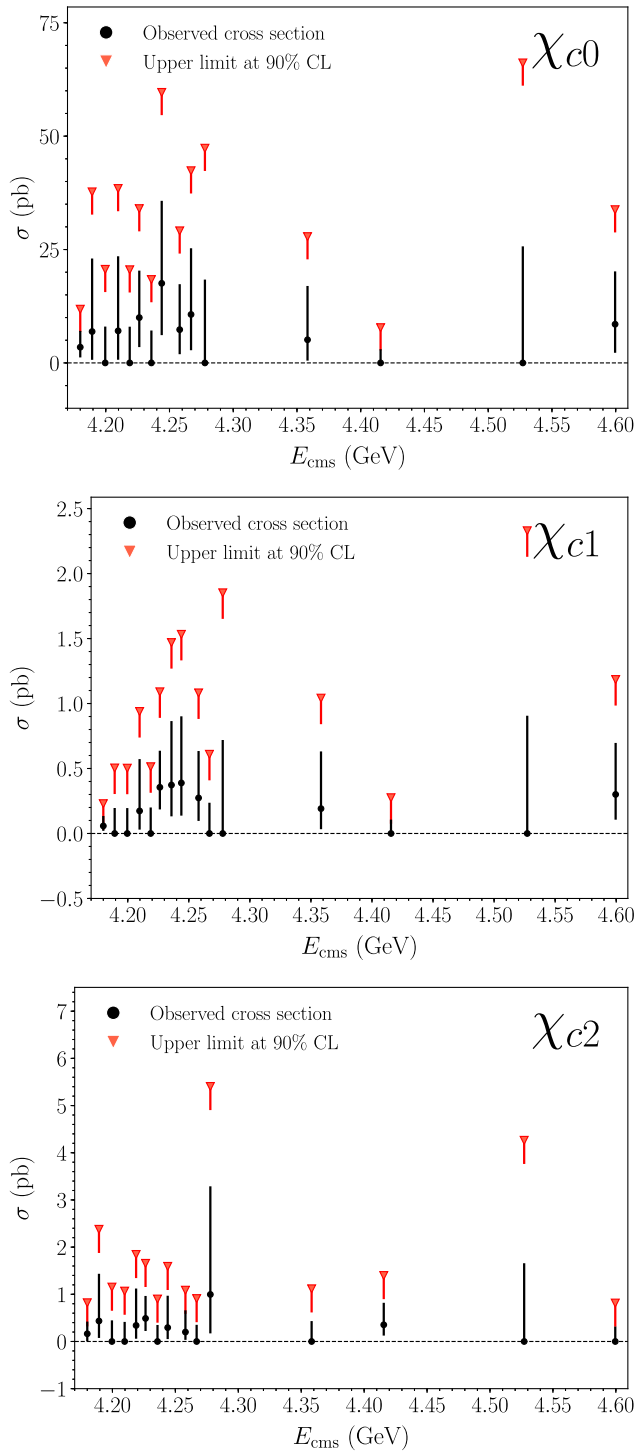

FIG. 4. Cross section (black) and corresponding upper limit (red) for the reaction channels $e^+e^- \to \chi_{cJ}\pi^+\pi^-$ versus the center-of-mass energy $E_{\rm cms}$.

IX. SUMMARY

We have performed a search for the process $e^+e^- \to \chi_{cJ}\pi^+\pi^-$, $\chi_{cJ} \to \gamma J/\psi$, $J/\psi \to (e^+e^-/\mu^+\mu^-)$, at center-of-mass energies ranging from 4.18 GeV to 4.60 GeV. No significant signal has been observed, despite the hint of an slight enhancement for $\pi^+\pi^-\chi_{c1}$ at center-of-mass energies between 4.18 GeV and 4.26 GeV. Thus, we set upper limits at the 90% CL for the three studied reaction channels for $J = 0$, 1, 2. Since no signal is observed also no charmoniumlike structure in the invariant mass of the $\chi_{cJ}\pi^{\pm}$ subsystem can be seen. So the upper limits of the reaction channels $\chi_{cJ}\pi^+\pi^-$ also apply for the case with an intermediate structure.

ACKNOWLEDGMENTS

The BESIII collaboration thanks the staff of BEPCII and the IHEP computing center for their strong support. This work is supported in part by National Key Basic Research Program of China under Contract No. 2015CB856700; National Natural Science Foundation of China (NSFC) under Contracts No. 11625523, No. 11635010, No. 11735014, No. 11822506, No. 11835012, No. 11935015, No. 11935016, No. 11935018, No. 11961141012; the Chinese Academy of Sciences (CAS) Large-Scale Scientific Facility Program; Joint Large-Scale Scientific Facility Funds of the NSFC and CAS under Contracts No. U1732263, No. U1832207; CAS Key Research Program of Frontier Sciences under Contracts No. QYZDJ-SSW-SLH003, No. QYZDJ-SSW-SLH040; 100 Talents Program of CAS; INPAC and Shanghai Key Laboratory for Particle Physics and Cosmology; ERC under Contract No. 758462; German Research Foundation DFG under Contracts Nos. Collaborative Research Center No. CRC 1044, FOR 2359; Istituto Nazionale di Fisica Nucleare, Italy; Ministry of Development of Turkey under Contract No. DPT2006K-120470; National Science and Technology fund; STFC (United Kingdom); The Knut and Alice Wallenberg Foundation (Sweden) under Contract No. 2016.0157; The Royal Society, UK under Contracts No. DH140054, No. DH160214; The Swedish Research Council; U.S. Department of Energy under Contracts No. DE-FG02-05ER41374, No. DE-SC-0012069; Olle Engkvist Foundation under Contract No. 200-0605.

[1] S. Godfrey and S. L. Olsen, Annu. Rev. Nucl. Part. Sci. **58**, 51 (2008).
[2] N. Brambilla *et al.*, Eur. Phys. J. C **71**, 1534 (2011).
[3] N. Brambilla *et al.*, Eur. Phys. J. C **74**, 2981 (2014).
[4] B. Aubert *et al.* (*BABAR* Collaboration), Phys. Rev. Lett. **95**, 142001 (2005).
[5] J. P. Lees *et al.* (*BABAR* Collaboration), Phys. Rev. D **86**, 051102 (2012).
[6] Q. He *et al.* (CLEO Collaboration), Phys. Rev. D **74**, 091104 (2006).
[7] C. Z. Yuan *et al.* (Belle Collaboration), Phys. Rev. Lett. **99**, 182004 (2007).
[8] Z. Q. Liu *et al.* (Belle Collaboration), Phys. Rev. Lett. **110**, 252002 (2013).
[9] M. Ablikim *et al.* (BESIII Collaboration), Phys. Rev. Lett. **110**, 252001 (2013).
[10] X. Mo, G. Li, C. Z. Yuan, K. L. He, H. M. Hu, J. H. Hu, P. Wang, and Z. Y. Wang, Phys. Lett. B **640**, 182 (2006).
[11] R. Mizuk *et al.* (Belle Collaboration), Phys. Rev. D **78**, 072004 (2008).
[12] J. P. Lees *et al.* (*BABAR* Collaboration), Phys. Rev. D **85**, 052003 (2012).
[13] S.-K. Choi *et al.* (Belle Collaboration), Phys. Rev. Lett. **100**, 142001 (2008).
[14] R. Aaij *et al.* (LHCb Collaboration), Phys. Rev. Lett. **112**, 222002 (2014).
[15] M. Ablikim *et al.* (BESIII Collaboration), Phys. Rev. Lett. **111**, 242001 (2013).
[16] M. Ablikim *et al.*, Nucl. Instrum. Methods Phys. Res., Sect. A **614**, 345 (2010).
[17] *BEPCII Performance and Beam Dynamics Studies on Luminosity*, edited by C. H. Yu *et al.*, IPAC2016 (Busan, Korea, 2016), http://accelconf.web.cern.ch/ipac2016/doi/JACoW-IPAC2016-TUYA01.html.
[18] X. L. Guo *et al.*, Radiat. Det. Technol. Methods **3**, 14 (2019).
[19] X. Li *et al.*, Radiat. Det. Technol. Methods **1**, 13 (2017).
[20] S. Agostinelli *et al.* (GEANT4 Collaboration), Nucl. Instrum. Methods Phys. Res., Sect. A **506**, 250 (2003).
[21] S. Jadach, B. Ward, and Z. Wąs, Comput. Phys. Commun. **130**, 260 (2000).
[22] D. J. Lange, Nucl. Instrum. Methods Phys. Res., Sect. A **462**, 152 (2001).
[23] E. Richter-Was, Phys. Lett. B **303**, 163 (1993).
[24] C. Patrignani *et al.* (Particle Data Group), Chin. Phys. C **40**, 100001 (2016).
[25] J. C. Chen, G. S. Huang, X. R. Qi, D. H. Zhang, and Y S. Zhu, Phys. Rev. D **62**, 034003 (2000).
[26] R. L. Yang, R. G. Ping, and C. Hong (BESIII Collaboration), Chin. Phys. Lett. **31**, 061301 (2014).
[27] M. Ablikim *et al.* (BESIII Collaboration), Chin. Phys. C **39**, 093001 (2015).
[28] M. Ablikim *et al.* (BESIII Collaboration), Phys. Rev. D **94**, 032009 (2016).
[29] M. Ablikim *et al.* (BESIII Collaboration), Phys. Rev. D **91**, 112005 (2015).
[30] M. Ablikim *et al.* (BESIII Collaboration), Phys. Rev. Lett. **114**, 092003 (2015).
[31] M. Ablikim *et al.* (BESIII Collaboration), Phys. Rev. D **93**, 011102 (2016).
[32] M. Ablikim *et al.* (BESIII Collaboration), Phys. Rev. D **99**, 091103 (2019).
[33] M. Ablikim *et al.* (BESIII Collaboration), Phys. Rev. Lett. **113**, 039903 (2014).
[34] M. Ablikim *et al.* (BESIII Collaboration), Phys. Rev. D **83**, 112005 (2011).
[35] E. Barberio, and Z. Wąs, Comput. Phys. Commun. **79**, 291 (1994).
[36] G. Montagna, M. Moretti, O. Nicrosini, and F. Piccinini, Nucl. Phys. **B541**, 31 (1999).
[37] R.-G. Ping, Chin. Phys. C **38**, 083001 (2014).
[38] R. D. Cousins, J. T. Linnemann, and J. Tucker, Nucl. Instrum. Methods Phys. Res., Sect. A **595**, 480 (2008).
[39] W. A. Rolke, A. M. Lopez, and J. Conrad, Nucl. Instrum. Methods Phys. Res., Sect. A **551**, 493 (2005).
[40] F. Jegerlehner, EPJ Web Conf. **218**, 10003 (2019).